

# Dynamic Neutrino Mass Ordering and Its Imprint on the Diffuse Supernova Neutrino Background

Yuber F. Perez-Gonzalez<sup>1,\*</sup> and Manibrata Sen<sup>2,†</sup>

<sup>1</sup>*Departamento de Física Teórica and Instituto de Física Teórica (IFT) UAM/CSIC, Universidad Autónoma de Madrid, Cantoblanco, 28049 Madrid, Spain*

<sup>2</sup>*Department of Physics, Indian Institute of Technology Bombay, Powai, Maharashtra 400076 India*

Neutrino masses may have evolved dynamically throughout the history of the Universe, potentially leading to a mass spectrum distinct from the normal or inverted ordering observed today. While cosmological measurements constrain the total energy density of neutrinos, they are not directly sensitive to a dynamically changing mass ordering unless future surveys achieve exceptional precision in detecting the distinct imprints of each mass eigenstate on large-scale structures. In this work, we investigate the impact of a dynamic neutrino mass spectrum on the diffuse supernova neutrino background (DSNB), which is composed of neutrinos from all supernova explosions throughout cosmic history and is on the verge of experimental detection. Since neutrino oscillations are highly sensitive to the mass spectrum, we show that the electron neutrino survival probability carries distinct signatures of the evolving neutrino mass spectrum. Our results indicate that the resulting modifications to the DSNB spectrum would exhibit unique energy-dependent features. These features are distinguishable from the effects of significant astrophysical uncertainties, providing a potential avenue for probing the dynamic nature of neutrino masses.

## I. INTRODUCTION

The neutrino remains the most elusive of the Standard Model (SM) particle content. Data from solar, atmospheric neutrino experiments as well as oscillation experiments have confirmed, beyond doubt, the presence of neutrino oscillations and hence non-zero masses. This confirmed our suspicion that the SM is incomplete, as the original framework does not account for neutrino mass.

Neutrino oscillation experiments measure the mass-squared difference associated with the solar sector,  $\Delta m_{\text{sol}}^2 = m_2^2 - m_1^2$ , as well as the absolute value of atmospheric mass-squared difference  $|\Delta m_{\text{atm}}^2| = |m_3^2 - m_1^2|$  [1]. Determination of the sign of  $\Delta m_{\text{atm}}^2$  is one of the major goals of neutrino physics. This information can be used to set limits on the sum of neutrino masses,  $\sum m_i \gtrsim 0.058 \text{ eV}$ ,  $i = 1, 2, 3$  in the Normal Mass Ordering (NO) or  $\sum m_i \gtrsim 0.1 \text{ eV}$  in the Inverted Mass Ordering (IO) [1]. Beta decay experiments like KATRIN can set an upper limit on the quantity,  $\sum_i \sqrt{|U_{ei}|^2 m_i^2} < 0.45 \text{ eV}$  (90% confidence level) [2], where  $U$  is the Pontecorvo–Maki–Nakagawa–Sakata mixing matrix.

The tiny mass of neutrinos also plays a role in the evolution of large-scale structures in the universe and can affect cosmic background radiation, providing clues about the early universe. The sum of neutrino masses ( $\sum_i m_i$ ) is also a critical parameter for cosmological models, affecting dark matter and energy density estimations. In fact, observations of the Cosmic Microwave Background by PLANCK restricts the sum to be  $\sum m_i < 0.26 \text{ eV}$  [3]. Recent data on the Baryonic Acoustic Oscillations (BAO) released from the Dark Energy Spectroscopic Instrument (DESI), combined with the Cosmic Microwave Background (CMB) data from PLANCK, have set  $\sum m_i < 0.072 \text{ eV}$  with 95% C.L [4]. This stringent limit casts doubt on the IO of neutrinos, ruling it out at a significance level of around  $3\sigma$ . Interestingly, the posterior probability distribution for  $\sum m_i$  peaks near zero (and can go to negative values of  $\sum m_i$  if positivity constraint is not imposed), *suggesting potential mild inconsistencies even with the NO* [5–7]. In fact, more recently, by integrating DESI BAO and CMB results with data from Supernova Ia, gamma-ray bursts (GRB), and X-ray observations, an even tighter constraint of  $\sum m_i < 0.043 \text{ eV}$  at the  $2\sigma$  C.L. has been established, thereby confirming the inconsistency [8].

The current experimental status on the measurement of the neutrino mass necessitates a revisiting of the mechanism of neutrino mass generation, which still remains a mystery. Several theoretical models of neutrino mass have been proposed, such as the see-saw mechanisms, which introduces either heavy right-handed neutrinos, or scalar triplets or fermionic triplets in the theory [9–14]. Models with additional discrete symmetries have also been explored in great detail [15]. The common link in the above theoretical models is that the neutrino mass arises due to a vacuum expectation value (vev) of a scalar particle (usually the Higgs). This is similar in spirit to the masses of the other SM fermions.

\* yuber.perez@uam.es

† manibrata@iitb.ac.in

However, neutrinos enjoy a special status in the SM fermion family and hence one can speculate that the neutrino mass has a totally different origin. This can either be due to any kind of novel phase transition in the early/late Universe [16–20], or due to interaction with some other particle, for e.g., dark matter [21–38]. A specific feature of these mass-models is that neutrino masses become redshift dependent. Therefore, neutrinos masses can be different in the early Universe from what is expected from current experiments. This might also provide a plausible explanation if the disagreement in  $\sum m_i$  between the oscillation experiments and the cosmological surveys persists.

It is important to emphasize at this stage that neutrino experiments can only probe the mass/mass-squared difference *today*. On the other hand, cosmological observables are actually sensitive to the neutrino energy density, which can be translated into the sum of the neutrino mass for non-relativistic neutrinos [39]. So, if the individual neutrino masses, or mass-ordering were different in the past, without violating the bound on the sum of neutrino masses from the CMB, cosmological surveys will have no way of probing it with the current/near future sensitivities.

This is where the Diffuse Supernova Neutrino Background (DSNB) can come in handy [40, 41]. This is composed of neutrinos coming from all possible core-collapse supernovae (SNe) from the time of star formation (redshift  $\sim 6$ ). Neutrinos produced inside SNe propagate through the dense matter before being emitted. Depending on the value and the sign of the mass-squared differences, neutrinos may undergo a Mikheyev-Smirnov-Wolfenstein (MSW) resonant flavor conversion during propagation inside the SN. The adiabaticity of crossing the resonance also depends on the mass-squared difference and the mixing angles. A change in the mass-squared difference or the mixing angle can lead to an observable change in the DSNB spectra. A detectable change in the DSNB spectra/flux can thus be used to probe such scenarios of dynamic neutrino mass generation [42]. Crucially, the expected change in the DSNB flux would not manifest as a simple normalization factor. Given that the mass generation mechanism ensures the neutrino spectrum observed today matches measurements, and it is possible that neutrinos were massless at higher redshifts, the final DSNB flux would result from a combination of SN fluxes produced under varying neutrino masses, each exhibiting distinct energy dependencies. Therefore, the resulting flux cannot be represented merely as a correction factor to the standard flux. This distinction implies that, in principle, one could differentiate flux modifications arising from mass-varying effects from those caused by astrophysical uncertainties, as the latter would alter the flux spectra in a qualitatively different manner. However, experimental limitations present significant challenges to detecting potential variations in neutrino masses across different redshifts.

The experimental landscape of DSNB detection seems very promising. The Super Kamiokande (SK), loaded with Gd, has been a front-runner in this quest. In fact, recently the collaboration reported a slight excess of events over over background in its Run VI and Run VII [43]. This excess, though in its nascent form, seems to be inconsistent with the theoretical predictions. Future runs will shed more light on this. Other promising experiments like the Jiangmen Underground Neutrino Observatory (JUNO), the Hyper-Kamiokande (HK) and the Deep Underground Neutrino Experiment (DUNE) will join the detection efforts within the next few years. While these experiments are mostly sensitive to  $\nu_e$  or  $\bar{\nu}_e$ , future dark matter detectors like DARWIN will also play an important role in detecting the non-electron flavor neutrinos. Theoretically, a number of works have demonstrated the potential of the DSNB to probe new physics scenarios, which causes a spectral distortion of the DSNB [44–50]. As a result, it is timely to visit the question of whether the DSNB can shed some light on the origins of neutrino mass.

This paper is organized as follows. In Section II, we consider the generalities of the DSNB flux, and its dependence on neutrino oscillations. Afterwards, we consider the model for varying neutrino mass ordering as function of redshift in Sec. III. We present our results in Sec. IV, and our conclusion in Sec. V. We use the natural units,  $\hbar = c = k_B = 1$ , throughout this manuscript.

## II. THE DIFFUSE SUPERNOVA NEUTRINO BACKGROUND

To predict the flux of the DSNB, it is essential to have a thorough understanding of the universe’s evolution, particularly focusing on the core-collapse SN (CCSN) rate, denoted as  $R_{\text{CCSN}}(z)$ , and the neutrino flavor dependent spectra from SNe,  $F_{\nu_\beta}$ . The rate of CCSN is directly tied to the star formation rate (SFR) throughout cosmic history, which has been assessed by several astronomical surveys [51–53]. The DSNB flux, without considering neutrino oscillations, can be expressed as,

$$\Phi_{\nu_\beta}^0(E) = \int_0^{z_{\text{max}}} \frac{dz}{H(z)} R_{\text{CCSN}}(z) F_{\nu_\beta}^0(E(1+z)), \quad (1)$$

where  $H(z)$  is the Hubble parameter and  $E$  is the neutrino energy today, adjusted with the redshift of emission. The maximum redshift for significant star formation activity is considered to be  $z_{\text{max}} \approx 6$ . The parameters needed for estimating  $R_{\text{CCSN}}(z)$  are taken from [41]. There are several sources of uncertainty that plague the determination of the DSNB flux, see Ref. [54] for a compendium of different sources of uncertainty. Since we are interested here in

demonstrating the effect of a redshift-dependent neutrino mass spectrum, we assume the uncertainty on the CCSN rate as the dominant one.

The unoscillated neutrino flux  $F_{\nu_\beta}^0(E)$  is a combination of contributions from both core-collapse SNe and black-hole-forming (BHF) failed supernovae such that

$$F_{\nu_\beta}^0(E) = f_{\text{SN}} F_{\nu_\beta}^{\text{SN}}(E_\nu) + f_{\text{BH}} F_{\nu_\beta}^{\text{BH}}(E_\nu), \quad (2)$$

where  $f_{\text{SN}}$  and  $f_{\text{BH}}$  represent the fractions of CCSNe and BHF events, respectively [55]. We consider in what follows  $f_{\text{BH}} = 0.21$ ,  $f_{\text{SN}} = 1 - f_{\text{BH}}$ . The functions  $F_{\nu_\beta}^{\text{SN}}$  and  $F_{\nu_\beta}^{\text{BH}}$  are the time-integrated spectra for core-collapse SNe and BHF-SNe. These spectra have been fitted using data from the Garching group simulations [56]. This comprehensive model allows us to estimate the DSNB flux by integrating over contributions from all past SNe, giving insights into the neutrino background that is a remnant of stellar evolution across cosmic time.

Neutrino propagation through a SN is influenced by the MSW flavor conversion, assuming that the mass-squared differences remain consistent with those measured in terrestrial experiments throughout cosmic history. However, the electron neutrino survival probability,  $P_{ee}$ , may vary as a function of redshift,  $z$ , for non-standard scenarios, as we will explore in this work. Consequently, the neutrino fluxes observed at Earth must incorporate this redshift dependence. Neglecting the effect of collective oscillations of neutrinos deep inside a SN, the fluxes can be expressed as follows

$$\Phi_{\nu_e}(E) = \int_0^{z_{\text{max}}} \frac{dz}{H(z)} R_{\text{CCSN}}(z) \{ P_{ee}(z) F_{\nu_e}^0 + [1 - P_{ee}(z)] F_{\nu_x}^0 \}, \quad (3a)$$

$$\Phi_{\bar{\nu}_e}(E) = \int_0^{z_{\text{max}}} \frac{dz}{H(z)} R_{\text{CCSN}}(z) \{ \overline{P_{ee}}(z) F_{\bar{\nu}_e}^0 + [1 - \overline{P_{ee}}(z)] F_{\nu_x}^0 \}, \quad (3b)$$

$$\Phi_{\nu_x}(E) = \int_0^{z_{\text{max}}} \frac{dz}{H(z)} R_{\text{CCSN}}(z) \frac{1}{4} \{ [1 - P_{ee}(z)] F_{\nu_e}^0 + [1 - \overline{P_{ee}}(z)] F_{\bar{\nu}_e}^0 + [2 + P_{ee}(z) + \overline{P_{ee}}(z)] F_{\nu_x}^0 \}. \quad (3c)$$

Here,  $F_{\nu_e}^0$ ,  $F_{\bar{\nu}_e}^0$ , and  $F_{\nu_x}^0$  represent the initial neutrino energy spectra for electron neutrinos, electron antineutrinos, and non-electron neutrinos, respectively, while  $\nu_x$  denotes all non-electronic flavors. Using these expressions, we now analyze a specific scenario in which the neutrino mass ordering has evolved over the history of the Universe, potentially leading to distinct imprints on the observed DSNB.

### III. DYNAMIC NEUTRINO MASS-SQUARED DIFFERENCES

The premise of our study is to probe the sensitivity of the DSNB spectra to dynamic neutrino mass-squared differences in the Universe. This can arise due to redshift dependent neutrino mass, which can be different for the different eigenstates. Such a scenario can either arise due to an unaccounted for phase transition as the Universe evolves, or due to neutrino interactions with dynamical dark energy or ultralight dark matter. In this work, we stay agnostic of the mechanism, and assume, for demonstration purpose, that the individual neutrino masses pick up a redshift dependence as follows,

$$m_i = m_i^\infty + \frac{m_i^0 - m_i^\infty}{1 + (z/z_i)^{B_i}}, \quad (4)$$

where  $m_i^0$  is the mass today and  $m_i^\infty$  is the mass at large redshifts. These two limits are joined by a smooth function, which transitions at  $z = z_i$ , with a rate governed by  $B_i$ , for each mass eigenstate  $i$ .

It is crucial to emphasize that the DSNB can be sensitive to dynamic (redshift dependent) neutrino masses, even if all the mass eigenstates transform at the same redshift,  $z_s$ , with the same rate,  $B_s$ . In that scenario, the sensitivity arises due to violation of adiabaticity in neutrino propagation as the masses become too small [42]. In this work, we generalize the scenario to the case where the redshift dependence is different for different eigenstates in a way that the neutrino mass ordering can be scrambled in the past. In this case, the mass-squared differences can become redshift-dependent and may even change sign in the past, significantly affecting neutrino flavor conversion in a highly dense environment such as a SN.

Once neutrinos decouple and begin to free-stream from the neutrinosphere during the cooling phase of a SN explosion, they propagate through regions of extremely high density,  $\rho \gg 10^{10} \text{ g cm}^{-3}$ . The flavor evolution of these neutrinos is governed by the mass-squared differences and the degree to which adiabatic conditions are satisfied. Under adiabatic propagation, neutrinos can undergo an MSW resonant conversion upon encountering the matter resonance

	$z_1$	$z_2$	$z_3$	$B_1$	$B_2$	$B_3$
NO	0.500	0.125	0.050	9	6	3
IO	0.125	0.125	0.500	6	3	9

TABLE I. Assumed values for the redshift dependence of the individual mass eigenstates.

density,  $\rho_{\text{res}}$ , defined as [57]

$$\rho_{\text{res}} = 1.4 \times 10^6 \text{ g cm}^{-3} \left( \frac{\Delta m^2}{1 \text{ eV}^2} \right) \left( \frac{10 \text{ MeV}}{E_\nu} \right) \cos 2\theta, \quad (5)$$

where  $\Delta m^2$  represents the relevant mass-squared difference,  $E_\nu$  is the neutrino energy, and  $\theta$  is the mixing angle. Two primary effects arise from changes in the mass-squared differences at earlier times. First, the sign of the mass-squared difference determines whether the resonance occurs for neutrinos or antineutrinos. Second, the magnitude of the mass-squared difference influences the adiabaticity of flavor propagation. Together, these effects alter the final flavor composition of neutrinos from a SN in a distinct way, leaving an imprint on the DSNB.

Generally, the electron neutrino survival probability can be estimated as follows. Inside the SN, within the high-density regions, the mixing between neutrino states becomes negligible, and the flavor states effectively coincide with the eigenstates in the medium. Specifically, for the electron flavor, we have:

$$\nu_e = \nu_h, \quad \bar{\nu}_e = \bar{\nu}_l, \quad (6)$$

where  $\nu_h$  ( $\bar{\nu}_l$ ) corresponds to the heaviest neutrino (lightest antineutrino) eigenstate in the medium at a given time. To estimate  $P_{ee}$ , we analyze the level-crossing diagrams, schematically illustrated in Fig. 1. These diagrams depict the eigenvalues of the Hamiltonian in constant matter as functions of the matter density, highlighting the regions where resonances occur based on the sign of the quadratic mass differences. As previously discussed, the occurrence of resonances for neutrinos or antineutrinos depends on the sign of the mass-squared differences. If the resonances are crossed adiabatically—that is, if the flip probability is negligible—the states will remain in their corresponding eigenstates in the medium. Under the assumption that adiabaticity conditions are satisfied for both resonances, whether for neutrinos or antineutrinos, the electron survival probabilities  $P_{ee}$  and  $\bar{P}_{ee}$  will be determined by the neutrino mixing matrix and can be expressed as:

$$P_{ee} = |U_{eh}|^2, \quad \bar{P}_{ee} = |U_{el}|^2, \quad (7)$$

where  $U_{eh}$  and  $U_{el}$  represent the elements of the mixing matrix associated with the heaviest and lightest eigenstates, respectively.

Given that the adiabaticity conditions may not have been satisfied in the Early Universe, we compute the survival probabilities of electron neutrinos and antineutrinos from a SN explosion at a given redshift  $z$  numerically. This calculation begins with tracking the flavor evolution within the SN by numerically solving the Schrödinger-like equations, using the assumed values of the mass splittings and mixing angles at that  $z$ , along with the electron density profile of the presupernova star, as provided in Ref. [56]. Following this, we model the propagation of neutrinos from the SN to Earth, taking into account the redshift-dependent evolution of neutrino masses. This step also involves solving the Schrödinger equations, but under vacuum conditions to account for the absence of significant matter effects during interstellar travel.

#### IV. RESULTS

We present in Fig. 2 the evolution of the neutrino masses (left panels), mass-squared differences (center), electron survival oscillation probabilities as measured at Earth for neutrinos and antineutrinos (right) assuming that today we have Normal (top) or Inverted (bottom) orderings. For these figures, we have chosen the values of  $z_i$  and  $B_i$  as given in Tab I. In the plots containing the mass splittings, we shaded the regions where the mass splittings become negative, and present in the insets the evolution of the absolute masses, with the lightest neutrino today having a mass of  $m_0 = 0.01 \text{ eV}$ . For the probability plots we shaded in gray the region in which the propagation inside the SN is non-adiabatic.

For the NO case today, we observe the standard case for  $z \lesssim 0.075$ , that is, the heaviest neutrino is  $\nu_3$  such that the

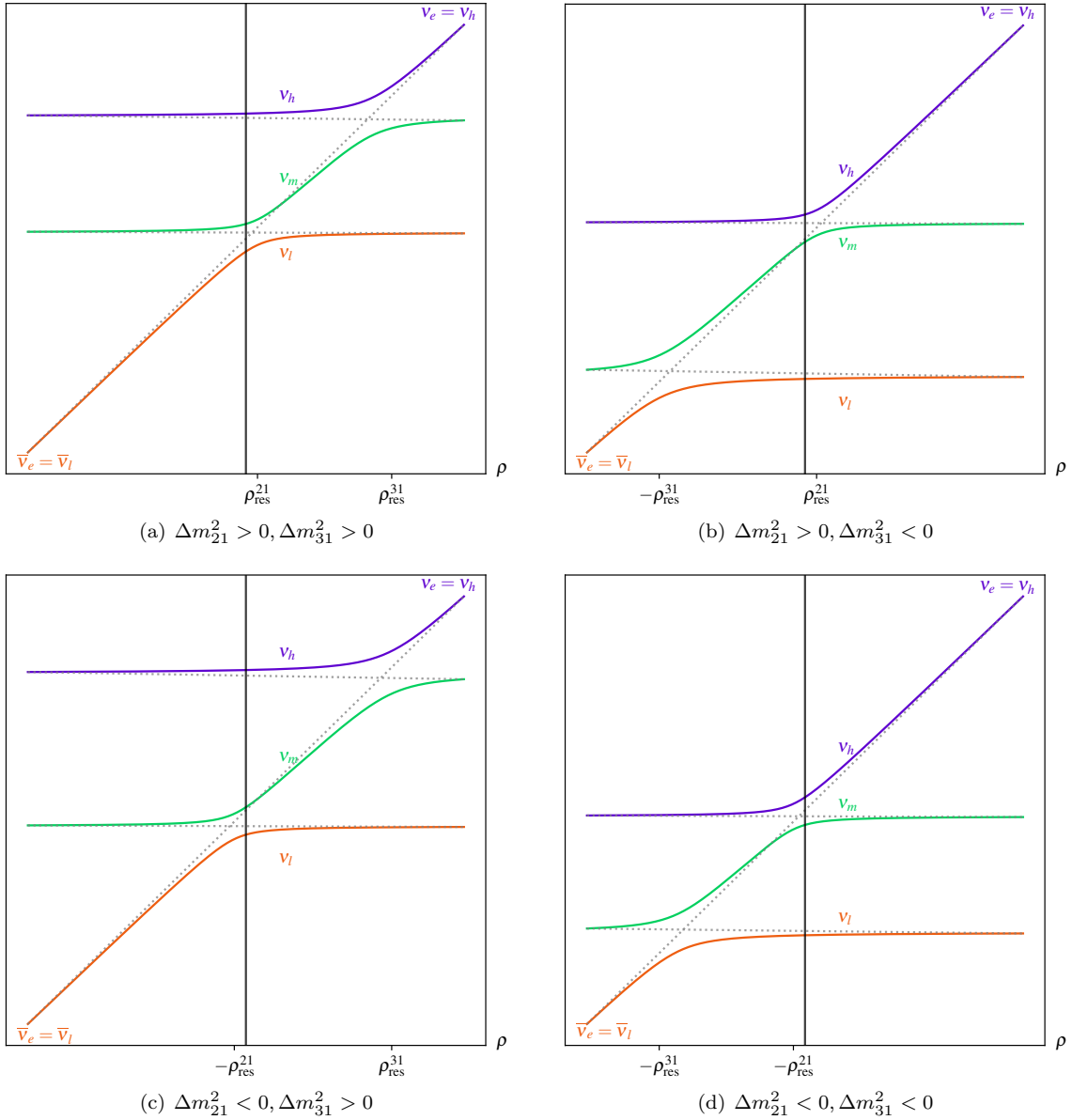


FIG. 1. Schematic depiction of level-crossing diagrams for neutrinos propagating through constant matter for different signs of the mass splittings as function of the density.  $\nu_{h,m,l}$  correspond to the heaviest, intermediate and lightest mass eigenstates in matter, respectively.  $\rho_{\text{res}}^{21}$ , and  $\rho_{\text{res}}^{31}$  refer to the values of densities that lead to a resonant enhancement of the flavor transformation for each mass splitting.

survival probability is  $|U_{e3}|^2$  for neutrinos. Once the neutrino masses start to change in redshift, we observe that the probability changes to  $P_{ee} = |U_{e2}|^2$ , as the atmospheric mass splitting becomes negative, causing the matter resonance to occur for antineutrinos rather than neutrinos. However, the solar mass splitting remains positive, enabling a MSW resonance that yields the observed probability. This occurs in the interval  $0.075 \lesssim z \lesssim 0.25$ . For larger redshifts,  $P_{ee} = |U_{e1}|^2$ , as both mass splittings become negative, preventing the occurrence of resonances for neutrinos, so that neutrinos propagate adiabatically  $\nu_e \leftrightarrow \nu_1$ . This will hold until the adiabaticity conditions are fulfilled, up to a value of  $z \sim 0.75$ . For larger values, the neutrino masses become negligible, so that the difference between the flavor and mass basis becomes unphysical, and the evolution inside the SN becomes trivial. Thus, once neutrinos obtain their masses during their propagation to Earth, they start oscillating, and quickly decohere. The survival probability as

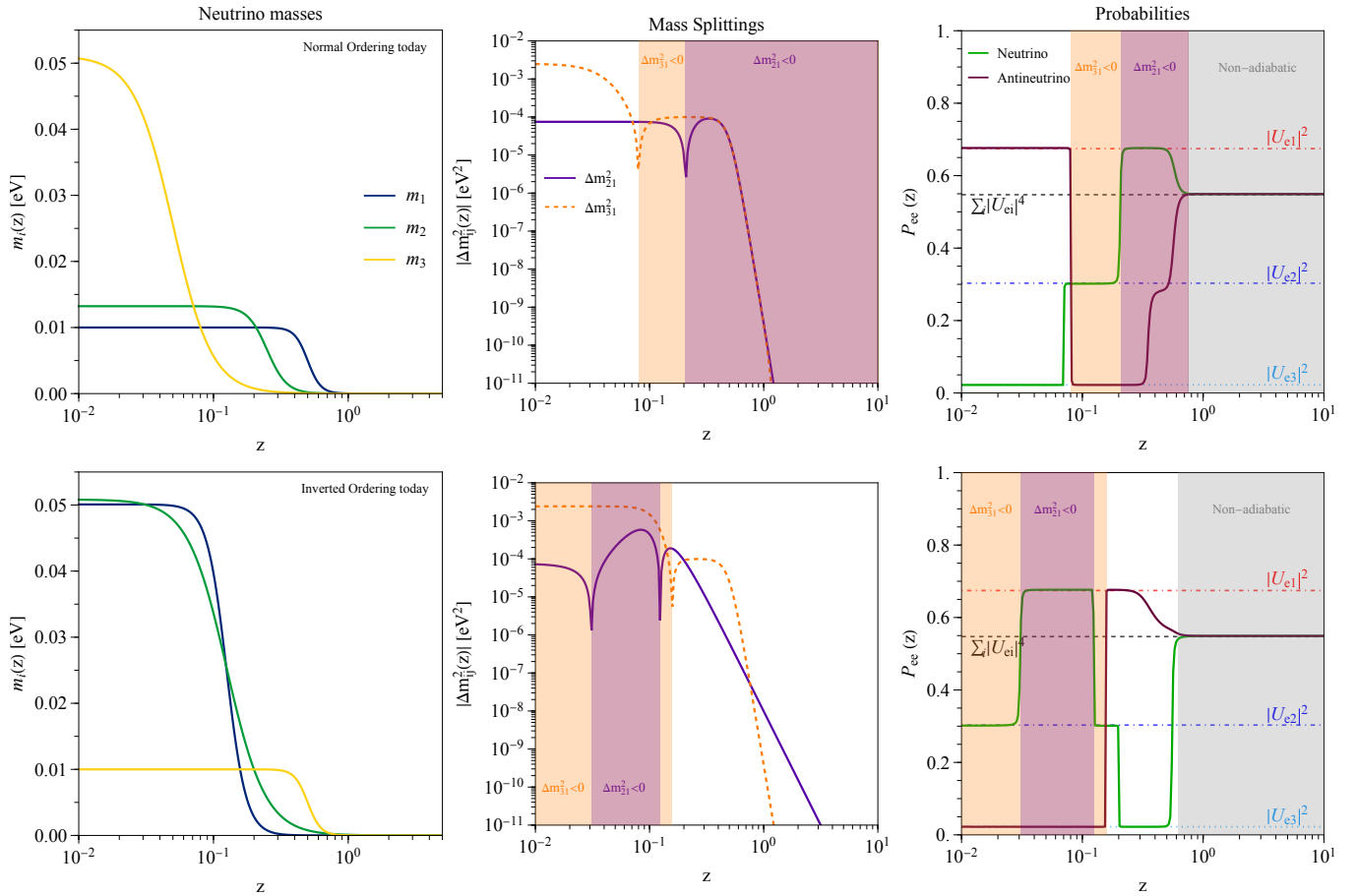


FIG. 2. Varying neutrino masses and mass splittings assuming NO (upper), IO (lower) today. We plot masses (left), quadratic mass differences (center) and electron survival probabilities  $P_{ee}$  at earth (right)

measured at Earth then is simple

$$P_{ee} = \sum_i |U_{ei}|^4 \sim 0.547. \quad (8)$$

For antineutrinos, we observe a similar behavior, with the difference that the probability depends on whether the mass splittings become negative, enabling the MSW resonances to occur inside the SN at a given  $z$ , provided that adiabaticity holds. For large redshifts  $z \gtrsim 0.75$ , when adiabaticity is violated, the probability tends to the same value as for neutrinos. Finally, in the case that the ordering is inverted today, we find that the probabilities for neutrinos and antineutrinos similarly depend on which is the heaviest or lightest eigenstate when the adiabatic conditions are fulfilled, respectively.

In Fig. 3, we present the resulting electron neutrino flux for the assumed parameters (blue), alongside the standard flux (white dashed line with orange shaded region indicating the uncertainty from the CCSN rate) and the unoscillated flux (orange dashed line). For neutrino energies  $E_\nu \lesssim 10$  MeV, the  $\nu_e$  flux in the NO scenario resembles the unoscillated flux, reduced by a factor of  $\sum_i |U_{ei}|^4 \sim 0.547$ . This behavior is expected because the DSNB flux at these energies is dominated by neutrinos emitted at redshifts  $z \gtrsim 1$ . At such redshifts, the assumed mass variations imply that neutrino masses were negligible, and the primary effect is decoherence as neutrinos begin to oscillate. At higher neutrino energies, however, the  $\nu_e$  flux deviates noticeably from both the unoscillated and standard DSNB fluxes. This deviation can be attributed to the dominance of the original  $\nu_x$  flux in the standard DSNB flux at Earth, which arises due to the small value of  $\theta_{13}$ . Since the  $\nu_x$  flux has a broader energy distribution, the  $\nu_e$  flux at Earth exceeds the unoscillated flux for  $E_\nu \gtrsim 15$  MeV. In the mass-varying scenario, the oscillation probability is larger than  $|U_{e3}|^2$ , leading to a more significant contribution from the original  $\nu_e$  flux at the neutrinosphere compared to the standard case. This alters the energy dependence of the flux at higher energies, reducing the flux below the region expected from the CCSN uncertainty, and modifying its power-law behavior. Such changes could be observable in future detections

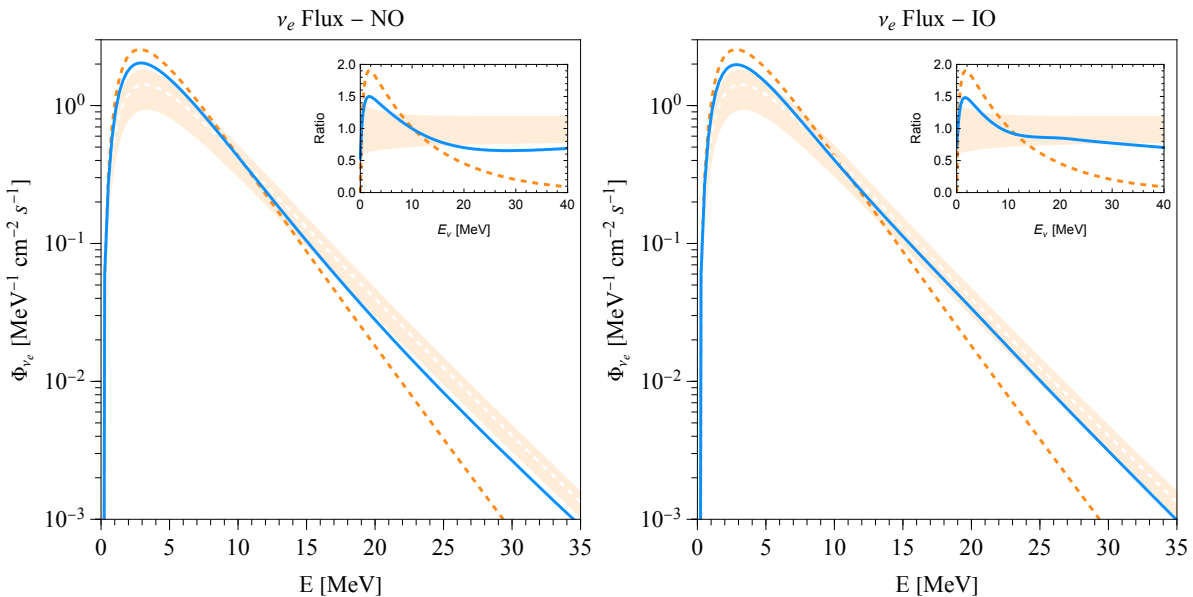


FIG. 3. Resulting DSNB fluxes for electron neutrinos as function of energy for NO (left) and IO (right) today for the benchmark cases presented in Tab. I (blue) and neglecting neutrino oscillations (dashed orange). The white dashed line indicates the standard neutrino flux assuming no variation of neutrino masses, and the orange band represents the uncertainty on the same flux due to the CCSN rate. The inset indicates the ratio of the fluxes to the standard flux.

of the  $\nu_e$  DSNB flux. To illustrate this energy-dependent behavior, Fig. 3 includes an inset showing the ratio of the unoscillated and mass-varying  $\nu_e$  fluxes to the standard case. This confirms the shift in the neutrino flux as a function of energy. A similar behavior is seen for the IO, with the main difference that the modified  $\nu_e$  flux at higher energies lies within the CCSN uncertainty band up to energies of  $E_\nu \gtrsim 35$  MeV. The corresponding  $\bar{\nu}_e$  flux does not change appreciably in the process, as explained in [42].

## V. CONCLUSION

The origin of the neutrino mass holds major clues to uncover the possible extensions of the Standard Model. While a number of theoretical possibilities exist, a confirmation can only be achieved after testing the predictions of the underlying models. A large number of terrestrial experiments lead the effort in trying to probe possible signatures arising out of models of neutrino masses. On the other hand, cosmological surveys take an indirect approach and try to probe the neutrino mass through its effect on structure formation.

This opens up the possibility of testing dynamic origins of neutrino masses, for example, neutrino masses from some unknown phase transitions in the early Universe, or neutrino masses due to coupling with some dynamic degrees of freedom. Often, in such models, neutrino masses pick up a redshift dependence and can be different in the past as compared to today. This offers an alternative mass mechanism to the usual vacuum expectation value driven neutrino masses. However, cosmological measurements of the neutrino mass rely on the neutrino density in the early Universe to probe their masses. As a result, these surveys are not sensitive to redshift dependent changes in the neutrino mass, as long as the energy density in the neutrinos remain the same.

In this work, we offer a complementary probe of dynamic redshift dependent neutrino masses in the early Universe using the Diffuse Supernova Neutrino Background (DSNB). The final flavor content of neutrinos emitted from a core-collapse supernova depends crucially on the details of neutrino propagation inside the supernova envelope. In particular, the sign of the mass-squared differences associated with the neutrinos determine whether a resonance is encountered by a neutrino or an antineutrino, and the value of the mass-squared differences determines whether the propagation is adiabatic. A combination of these two effects determine the neutrino flavor arriving at the Earth. Hence, any dynamic changes in the neutrino masses, and hence mass-orderings, will be imprinted on the DSNB. This, of course, requires that the neutrino masses change considerably within the redshift of star formation ( $z \lesssim 6$ ). However,

We demonstrated this idea by considering simple toy models of redshift dependent neutrino masses, without alluring to any specific model. We considered the generic case where each of the neutrino masses can have a different redshift

dependence. This can lead to scenarios where the mass-orderings in the past becomes different from what it is today. Numerically solving for the neutrino propagation inside a supernova for such different scenarios, we analyzed the differences that can arise in the DSNB. We found that the overall effect is not just a change in the normalization of the DSNB, but an alteration of the energy dependence. In optimistic cases, the changes can lie even below the current uncertainties and offer a potential target for future DSNB searches.

We would like to conclude by emphasizing the potential of the DSNB to probe the nature of the neutrino masses. If neutrino masses indeed have a dynamic nature, the only feasible way of testing this directly is through the DSNB. One can, in principle, have some imprints of this in large scale structures as well, however, the sensitivity required to probe these effects is beyond the reach of even next generation experiments. This makes the DSNB the only way of testing the dynamic nature of neutrino masses directly.

## ACKNOWLEDGEMENTS

We thank Enrique Fernández-Martínez, Joachim Kopp, Daniel Naredo, Ivan Martínez-soler and Tim Herbermann for useful discussions. We also thank Augustine Paulaner for insightful discussions which led to the idea that shaped the manuscript. YFPG acknowledges financial support by the Consolidación Investigadora grant CNS2023-144536 from the Spanish Ministerio de Ciencia e Innovación (MCIN) and by the Spanish Research Agency (Agencia Estatal de Investigación) through the grant IFT Centro de Excelencia Severo Ochoa No CEX2020-001007-S. We would also like to thank the Galileo Galilei Institute for Theoretical Physics for the hospitality and the INFN for partial support during the completion of this work.

- 
- [1] S. Navas *et al.* (Particle Data Group), *Phys. Rev. D* **110**, 030001 (2024).
  - [2] M. Aker *et al.* (Katrin), (2024), arXiv:2406.13516 [nucl-ex].
  - [3] N. Aghanim *et al.* (Planck), *Astron. Astrophys.* **641**, A6 (2020), [Erratum: *Astron. Astrophys.* 652, C4 (2021)], arXiv:1807.06209 [astro-ph.CO].
  - [4] A. G. Adame *et al.* (DESI), (2024), arXiv:2404.03002 [astro-ph.CO].
  - [5] N. Craig, D. Green, J. Meyers, and S. Rajendran, *JHEP* **09**, 097 (2024), arXiv:2405.00836 [astro-ph.CO].
  - [6] D. Green and J. Meyers, (2024), arXiv:2407.07878 [astro-ph.CO].
  - [7] D. Naredo-Tuero, M. Escudero, E. Fernández-Martínez, X. Marciano, and V. Poulin, *Phys. Rev. D* **110**, 123537 (2024), arXiv:2407.13831 [astro-ph.CO].
  - [8] D. Wang, O. Mena, E. Di Valentino, and S. Gariazzo, *Phys. Rev. D* **110**, 103536 (2024), arXiv:2405.03368 [astro-ph.CO].
  - [9] P. Minkowski, *Phys. Lett. B* **67**, 421 (1977).
  - [10] M. Gell-Mann, P. Ramond, and R. Slansky, *Conf. Proc. C* **790927**, 315 (1979), arXiv:1306.4669 [hep-th].
  - [11] T. Yanagida, *Conf. Proc. C* **7902131**, 95 (1979).
  - [12] R. N. Mohapatra and G. Senjanovic, *Phys. Rev. Lett.* **44**, 912 (1980).
  - [13] R. N. Mohapatra and G. Senjanovic, *Phys. Rev. D* **23**, 165 (1981).
  - [14] J. Schechter and J. W. F. Valle, *Phys. Rev. D* **22**, 2227 (1980).
  - [15] S. F. King and C. Luhn, *Rept. Prog. Phys.* **76**, 056201 (2013), arXiv:1301.1340 [hep-ph].
  - [16] R. Fardon, A. E. Nelson, and N. Weiner, *JCAP* **10**, 005 (2004), arXiv:astro-ph/0309800.
  - [17] S. M. Kocsbang and S. Hannestad, *JCAP* **09**, 014 (2017), arXiv:1707.02579 [astro-ph.CO].
  - [18] G. Dvali and L. Funcke, *Phys. Rev. D* **93**, 113002 (2016), arXiv:1602.03191 [hep-ph].
  - [19] C. S. Lorenz, L. Funcke, E. Calabrese, and S. Hannestad, *Phys. Rev. D* **99**, 023501 (2019), arXiv:1811.01991 [astro-ph.CO].
  - [20] C. S. Lorenz, L. Funcke, M. Löffler, and E. Calabrese, *Phys. Rev. D* **104**, 123518 (2021), arXiv:2102.13618 [astro-ph.CO].
  - [21] A. Berlin, *Phys. Rev. Lett.* **117**, 231801 (2016), arXiv:1608.01307 [hep-ph].
  - [22] G. Krnjaic, P. A. N. Machado, and L. Necib, *Phys. Rev. D* **97**, 075017 (2018), arXiv:1705.06740 [hep-ph].
  - [23] V. Brdar, J. Kopp, J. Liu, P. Prass, and X.-P. Wang, *Phys. Rev. D* **97**, 043001 (2018), arXiv:1705.09455 [hep-ph].
  - [24] F. Capozzi, I. M. Shoemaker, and L. Vecchi, *JCAP* **07**, 004 (2018), arXiv:1804.05117 [hep-ph].
  - [25] K.-Y. Choi, E. J. Chun, and J. Kim, *Phys. Dark Univ.* **30**, 100606 (2020), arXiv:1909.10478 [hep-ph].
  - [26] A. Dev, P. A. N. Machado, and P. Martínez-Miravé, *JHEP* **01**, 094 (2021), arXiv:2007.03590 [hep-ph].
  - [27] K.-Y. Choi, E. J. Chun, and J. Kim, (2020), arXiv:2012.09474 [hep-ph].
  - [28] S.-F. Ge, *J. Phys. Conf. Ser.* **1468**, 012125 (2020).
  - [29] M. Losada, Y. Nir, G. Perez, and Y. Shpilman, *JHEP* **04**, 030 (2022), arXiv:2107.10865 [hep-ph].
  - [30] G.-y. Huang and N. Nath, *JCAP* **05**, 034 (2022), arXiv:2111.08732 [hep-ph].
  - [31] E. J. Chun, (2021), arXiv:2112.05057 [hep-ph].
  - [32] A. Dev, G. Krnjaic, P. Machado, and H. Ramani, *Phys. Rev. D* **107**, 035006 (2023), arXiv:2205.06821 [hep-ph].
  - [33] G.-y. Huang, M. Lindner, P. Martínez-Miravé, and M. Sen, *Phys. Rev. D* **106**, 033004 (2022), arXiv:2205.08431 [hep-ph].
  - [34] H. Davoudiasl and P. B. Denton, (2023), arXiv:2301.09651 [hep-ph].

- [35] M. Losada, Y. Nir, G. Perez, I. Savoray, and Y. Shpilman, (2023), arXiv:2302.00005 [hep-ph].
- [36] M. Sen and A. Y. Smirnov, *JCAP* **01**, 040 (2024), arXiv:2306.15718 [hep-ph].
- [37] M. Sen and A. Y. Smirnov, (2024), arXiv:2407.02462 [hep-ph].
- [38] P. Martínez-Miravé, Y. F. Perez-Gonzalez, and M. Sen, *Phys. Rev. D* **110**, 055005 (2024), arXiv:2406.01682 [hep-ph].
- [39] J. Lesgourgues and S. Pastor, *Adv. High Energy Phys.* **2012**, 608515 (2012), arXiv:1212.6154 [hep-ph].
- [40] C. Lunardini, *Astropart. Phys.* **26**, 190 (2006), arXiv:astro-ph/0509233.
- [41] J. F. Beacom, *Ann. Rev. Nucl. Part. Sci.* **60**, 439 (2010), arXiv:1004.3311 [astro-ph.HE].
- [42] A. de Gouvêa, I. Martinez-Soler, Y. F. Perez-Gonzalez, and M. Sen, *Phys. Rev. D* **106**, 103026 (2022), arXiv:2205.01102 [hep-ph].
- [43] M. Harada, “Review of diffuse sn neutrino background,” (2024).
- [44] A. De Gouvêa, I. Martinez-Soler, Y. F. Perez-Gonzalez, and M. Sen, *Phys. Rev. D* **102**, 123012 (2020), arXiv:2007.13748 [hep-ph].
- [45] Z. Tabrizi and S. Horiuchi, *JCAP* **05**, 011 (2021), arXiv:2011.10933 [hep-ph].
- [46] K. Akita, S. H. Im, and M. Masud, *JHEP* **12**, 050 (2022), arXiv:2206.06852 [hep-ph].
- [47] A. Das, T. Herbermann, M. Sen, and V. Takhistov, *JCAP* **07**, 045 (2024), arXiv:2403.15367 [hep-ph].
- [48] P. Ivanov-Ballesteros and M. C. Volpe, *Phys. Rev. D* **107**, 023017 (2023), arXiv:2209.12465 [hep-ph].
- [49] M. MacDonald, P. Martínez-Miravé, and I. Tamborra, *JCAP* **01**, 062 (2025), arXiv:2409.16367 [astro-ph.HE].
- [50] I. R. Wang, X.-J. Xu, and B. Zhou, (2025), arXiv:2501.07624 [hep-ph].
- [51] A. M. Hopkins and J. F. Beacom, *Astrophys. J.* **651**, 142 (2006), arXiv:astro-ph/0601463 [astro-ph].
- [52] H. Yuksel, M. D. Kistler, J. F. Beacom, and A. M. Hopkins, *Astrophys. J.* **683**, L5 (2008), arXiv:0804.4008 [astro-ph].
- [53] S. Horiuchi, J. F. Beacom, and E. Dwek, *Phys. Rev.* **D79**, 083013 (2009), arXiv:0812.3157 [astro-ph].
- [54] D. Kresse, T. Ertl, and H.-T. Janka, *Astrophys. J.* **909**, 169 (2021), arXiv:2010.04728 [astro-ph.HE].
- [55] K. Møller, A. M. Suliga, I. Tamborra, and P. B. Denton, *JCAP* **1805**, 066 (2018), arXiv:1804.03157 [astro-ph.HE].
- [56] “Results from an extended set of 1d core-collapse simulations for a variety of progenitors can be found at,” <https://www.mpa.mpg.de/ccsnarchive/>, Accessed: 2010-09-30.
- [57] A. S. Dighe and A. Yu. Smirnov, *Phys. Rev.* **D62**, 033007 (2000), arXiv:hep-ph/9907423 [hep-ph].